Effective Photo- and Triboluminescent Eu^{III} Coordination Polymers with Rigid Triangular Spacer Ligands

Yasuchika Hasegawa,*[a] Shiori Tateno,[b] Masanori Yamamoto,[b] Takayuki Nakanishi,[a] Yuichi Kitagawa, [a] Tomohiro Seki, [a] Hajime Ito[a] and Koji Fushimi[a]

Abstract: Luminescent Eu^{III} coordination polymers with rigid triangular spacer ligands are reported. The Eu^{III} coordination polymer, $[Eu_3(hfa)_9(tppb)_2]_n$ (hfa: hexafluoroacetylacetonate, tppb: tris(4-diphenylphosphorylphenyl)benzene), shows high thermo-stability (decomposition temperature = 354˚C) and photoluminescence quantum yield ($\Phi_{4f\text{-}4f}$ = 82%, photosensitized energy transfer efficiency = 78%). The triboluminescence efficiency of Eu(III) coordination polymer with triangular spacers under laser pulse irradiation (Nd: YAG, λ = 1064 nm, pulse width = 5 ns, pulse energy = 0.1 mJ) is calculated to be 49%. Characteristic triangular structure, high emission quantum yield, effective photosensitized energy transfer and remarkable triboluminescence properties of Eu(III) coordination polymers are demonstrated for the first time.

Introduction

Coordination polymers composed of metal ions and organic joint ligands have attracted considerable attention in the fields of coordination chemistry, inorganic chemistry, supramolecular chemistry, polymer and material science.[1-5] One-, two- and three-dimensional alternating sequences of metal ions and organic ligands exhibit remarkable characteristics as novel organic–inorganic hybrid materials with various structures, and unique physical properties that can be easily prepared by the combination of metal ions and organic ligands. We here focus on coordination polymers formed with luminescent lanthanide ions, lanthanide coordination polymers.[6] Lanthanide coordination polymers are regarded as attractive luminescent materials because of their characteristic narrow emission bands (full width at half-maximum, fwhm < 10 nm), wide emission area (UV/Vis/near-IR) and long emission lifetimes (τ > ms), based on the 4*f*–4*f* transitions. In particular, The Eu^{III} and Tb^{III} coordination polymers are promising monochromatic red and green luminescent materials, respectively, for display and sensing devices.[7,8]

Lanthanide coordination polymers are generally constructed from lanthanide ions and small organic joint parts with two coordination sites. The carboxylic group is a typical functional group that acts as a coordination site for the formation of lanthanide coordination polymers. Daiguebonne and Bünzli reported micro- and nanosized particles of lanthanide coordination polymers linked with benzene-*p*-dicarboxylates.[9] The Tb^{III}-containing coordination polymers exhibit large emission quantum yields up to 43%. Bettencourt-Dias presented two-dimensional coordination polymers composed of lanthanide ions and benzene-m-dicarboxylates (isophthalic acid) or thiophene-derivatized isophthalic acid, where the emission quantum yields of the excited Tb^{III} coordination polymers with a π-π^* transition were estimated to be 3.6 and 7.5%, respectively.[10] Lanthanide coordination polymers linked with tricarboxylate ligands (benzene and pyridine-2,4,6-tricarboxylate) were reported by Cheng and coworkers.[11] We have reported luminescent lanthanide coordination polymers linked with bidentate phosphine oxide groups.[12] The bidentate phosphine oxide groups are linked with organo-aromatic compounds. The vibrational frequency of phosphine oxide (P=O: 1125 cm^{-1}) is smaller than that of the carboxylic group (C=O: ca. 1600 cm^{-1}). The smaller vibrational frequency of the coordination site in lanthanide complexes and coordination polymers leads to the suppression of vibrational relaxation from the excited state, which results in a smaller non-radiative rate constant (k_{nr}) and a higher emission quantum yield.[13] Combination of bidentate phosphine oxide and low-vibrational $Eu(hfa)_3$ (hfa: hexafluoroacetylacetonate) units are effective for the preparation of strongly luminescent lanthanide coordination polymers that exhibit large emission quantum yields up to 70% under 4*f*–4*f* excitation.[12]

In this study, we designed novel Eu^{III} coordination polymers with rigid triangular spacer ligands for effective photo- and triboluminescence (Figure 1a and b). Triboluminescence is the emission of light originating from mechanical stress on bulk solid materials.[14, 15] Molecular crystals composed of lanthanide complexes and coordination polymers have been studied for effective triboluminescence, recenlty.[16-20] While there have been extensive discussions on the origin of triboluminescence from molecular crystals, some studies have indicated a contribution of the piezoelectric effect upon breaking non-centrosymmetric bulk crystals.[21] The Eu^{III} coordination polymers with triangular spacers in Figure 1a and b are expected to provide close packed structures and effective crystal cracking under mechanical stress. The Eu^{III} coordination polymers are composed of luminescent $Eu(hfa)_3$ (hfa: hexafluoroacetylacetonate) parts[13] and novel tridentate phosphine oxides ligands, tris(4-diphenylphosphorylphenyl)benzene (tppb) and tris(4-diphenylphosphorylphenyl)-1,3,5-triazine (tpptz). Based on the

[a] Prof. Dr. Y. Hasegawa, Dr. T. Nakanishi, Dr. Y. Kitagawa, Dr. T. Seki, Prof. Dr. H. Ito, Dr. K. Fushimi
Faculty of Engineering, Hokkaido University, Kita-13 Jo, Nishi-8 Chome, Kita-ku, Sapporo, Hokkaido, 060-8628 (Japan)
E-mail: hasegaway@eng.hokudai.ac.jp
[b] S. Tateno, M. Yamamoto
Graduate School of Chemical Sciences and Engineering, Hokkaido University, Kita-13 Jo, Nishi-8 Chome, Kita-ku, Sapporo, Hokkaido, 060-8628 (Japan)

Supporting information for this article is given via a link at the end of the document.

their elemental analyses, ratio of $Eu(hfa)_3$ and triangular spacer was estimated to be 2:3. One-dimensional Eu^{III} coordination polymer with dpbp (4,4-Bis(diphenylphosphoryl)biphenyl) was also prepared as a standard reference (Figure 1c). Their emission quantum yields can be quantitatively estimated using the radiative and non-radiative rate constants calculated from the emission spectrum and lifetime.[22, 23] We also estimated triboluminescence properties of one- and Eu^{III} coordination polymers under shock wave irradiation using Nd:YAG nano-second pulse laser. Shock wave irradiation should be effective for quick crushing of the crystals, resulting in observation of the emission spectrum and lifetime from the crushing point or face on the Eu^{III} coordination polymers. Triboluminescence analysis of sugar powders using shock wave laser irradiation in the near-infrared region according to the source of mechanical stress have been also reported.[24] In the present study, photo- and triboluminescence properties of Eu^{III} coordination polymers with triangular spacers are demonstrated for the first time.

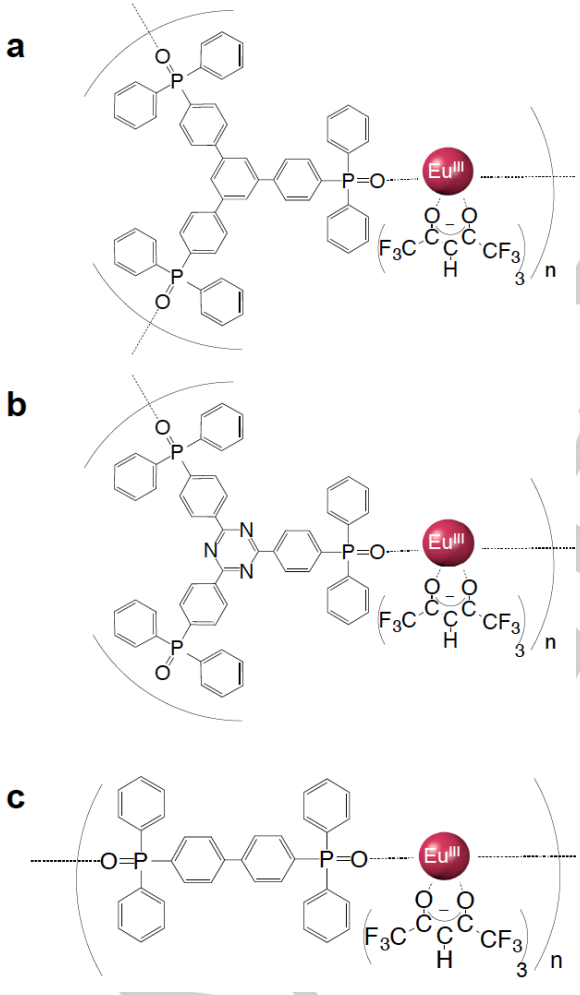

Figure 1. Chemical structures of (a) $[Eu_3(hfa)_9(tppb)_2]_n$, (b) $[Eu_3(hfa)_9(tpptz)_2]_n$, and (c) $[Eu(hfa)_3(dpbp)]_n$

Results and Discussion

Structural properties

The Eu^{III} coordination polymers, $[Eu_3(hfa)_9(tppb)_2]_n$ and $[Eu_3(hfa)_9(tpptz)_2]_n$, were prepared by the complexation of $Eu(hfa)_3(H_2O)_2$ with the corresponding tridentate phosphine oxide ligands. The X-ray single crystal data of the tppb and tpptz derivatives are shown in the Supporting Information (Figure S1, S2 and Table S1). Naik and co-workers have reported a π-π stacking interaction between triazine-linked tpptz derivatives.[25] Eu^{III} coordination polymers attached with tppb and tpptz ligands might be formed the tight packing structures in the crystals.

The polymeric structures of $[Eu_3(hfa)_9(tppb)_2]_n$ and $[Eu_3(hfa)_9(tpptz)_2]_n$ were characterized using ESI-MS. The observed ESI-MS signals of $[Eu_3(hfa)_9(tpptz)_2]_n$ are shown in Figure 2. The observed signals with mass numbers (m/z) of 1476.12, 2249.49, 3024.91 and 3933.07 were assigned to fragments $[Eu(hfa)_2(tpptz)]^+$, $[Eu_2(hfa)_5(tpptz)]^+$, $[Eu_3(hfa)_8(tpptz)_3]^+$ and $[Eu_3(hfa)_8(tpptz)_2]^+$, respectively. The assignment was made by comparing the observed isotope distribution of $[Eu(hfa)_2(tpptz)]^+$ (m/z at around 1476.12) with the caluculated data. We also found that signals with mass numbers (m/z) of 1410.13, 2379.40, 3286.62, 4059.45 and 4833.38 were attributed to fragments $[Eu(hfa)_2(tppb)]^+$, $[Eu(hfa)_2(tppb)_2]^+$, $[Eu(hfa)_2(tppb)_3]^+$, $[Eu_2(hfa)_5(tppb)_3]^+$ and $[Eu_3(hfa)_8(tppb)_3]^+$, respectively.

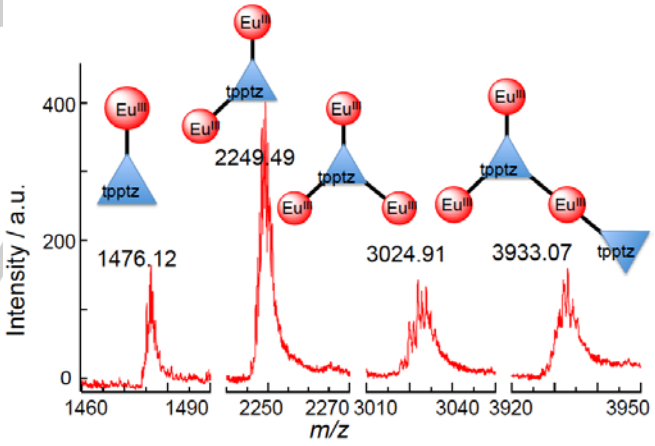

Figure 2. ESI-MS spectrum of $[Eu_3(hfa)_9(tpptz)_2]_n$ using methanol.

The structures of prepared $[Eu_3(hfa)_9(tppb)_2]_n$ and $[Eu_3(hfa)_9(tpptz)_2]_n$ were also characterized using powder XRD measurements. These XRD spectra are shown in Figure 3a. Peaks for $[Eu_3(hfa)_9(tppb)_2]_n$ were observed at 14.56˚, 16.30˚, 16.89˚, 19.60˚, 20.12˚, 21.05˚, 21.90˚, 23.42˚, 24.37˚ (Figure 3a: red- line 1), which is similar to those for $[Eu_3(hfa)_9(tpptz)_2]_n$, 14.31˚, 15.62˚, 17.02˚, 18.35˚, 20.17˚, 20.90˚, 21.30˚, 22.00˚, 23.60˚, 24.08˚ (Figure 3a: blue-line 2). These peaks of $[Eu_3(hfa)_9(tppb)_2]_n$ and $[Eu_3(hfa)_9(tpptz)_2]_n$ are much different from that of one-dimensional Eu^{III} coordination polymer

$[Eu(hfa)_3(dpbp)]_n$. The peaks of Eu^{III} coordination polymers with trianglar spacers might affected by tight packing in the crystals.

The thermal stability of $[Eu_3(hfa)_9(tppb)_2]_n$ and $[Eu_3(hfa)_9(tpptz)_2]_n$ were evaluated using TGA (Figure 3b and Table 1). The decomposition temperatures for $[Eu_3(hfa)_9(tppb)_2]_n$ and $[Eu_3(hfa)_9(tpptz)_2]_n$ were estimated to be 354˚C and 355˚C, respectively. These decomposition temperatures are higher than that of corresponding previous $[Eu(hfa)_3(dpbp)]_n$ (decomposition temperature = 308˚C).[12] The increase in the decomposition temperatures of $[Eu_3(hfa)_9(tppb)_2]_n$ and $[Eu_3(hfa)_9(tpptz)_2]_n$ is caused by tight packing structures of Eu^{III} coordination polymers.

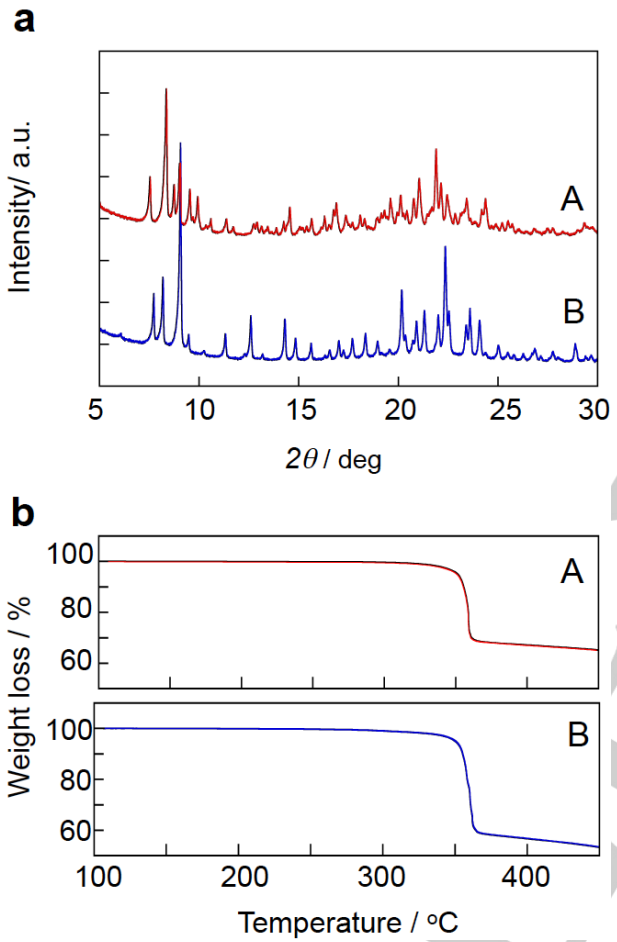

Figure 3. (a) XRD patterns of A: $[Eu_3(hfa)_9(tppb)_2]_n$ and B: $[Eu_3(hfa)_9(tpptz)_2]_n$ (b) TGA curves of A: $[Eu_3(hfa)_9(tppb)_2]_n$ and B: $[Eu_3(hfa)_9(tpptz)_2]_n$ in an argon atmosphere at a heating rate of 5 ˚C min^{-1}.

Photoluminescence properties

In order to estimate electronic structures of tppb and tpptz ligands in solid Eu^{III} coordination polymers, diffuse-reflectance absorption spectra of $[Eu_3(hfa)_9(tppb)_2]_n$ and $[Eu_3(hfa)_9(tpptz)_2]_n$ were measured. These spectra are shown in Figure 4a and b (solid line). The absorption shoulder bands at 300 nm are attributed to π-π^* transitions of the hfa ligands in $[Eu_3(hfa)_9(tppb)_2]_n$ and $[Eu_3(hfa)_9(tpptz)_2]_n$, which agree with the absorption band of $[Eu(hfa)_3(H_2O)_2]$ at around 300 nm. The absorption bands at around 340 nm (solid line) are due to triangular spacers, tppb and tpptz (dashed lines). We found remarkable absorption shoulder bands of solid state $[Eu_3(hfa)_9(tppb)_2]_n$ at around 400 nm, although absorption bands at around 400 nm were not observed in solid state $[Eu(hfa)_3(H_2O)_2]$, $[Eu(hfa)_3(tppo)_2]$ (tppo: monodentate triphenyl phosphine oxide),[26] tppb or tpptz (dashed lines). The characteristic absorption shoulder band could be assigned to the interligand charge transfer (ILCT) via charge re-distribution of the hfa ligands.[19] The ILCT state via charge redistribution is formed in close packing crystals.[27] Observation of the characteristic bands at around 350 nm in solid is significant for formation of close packing structures in $[Eu_3(hfa)_9(tppb)_2]_n$ crystals.

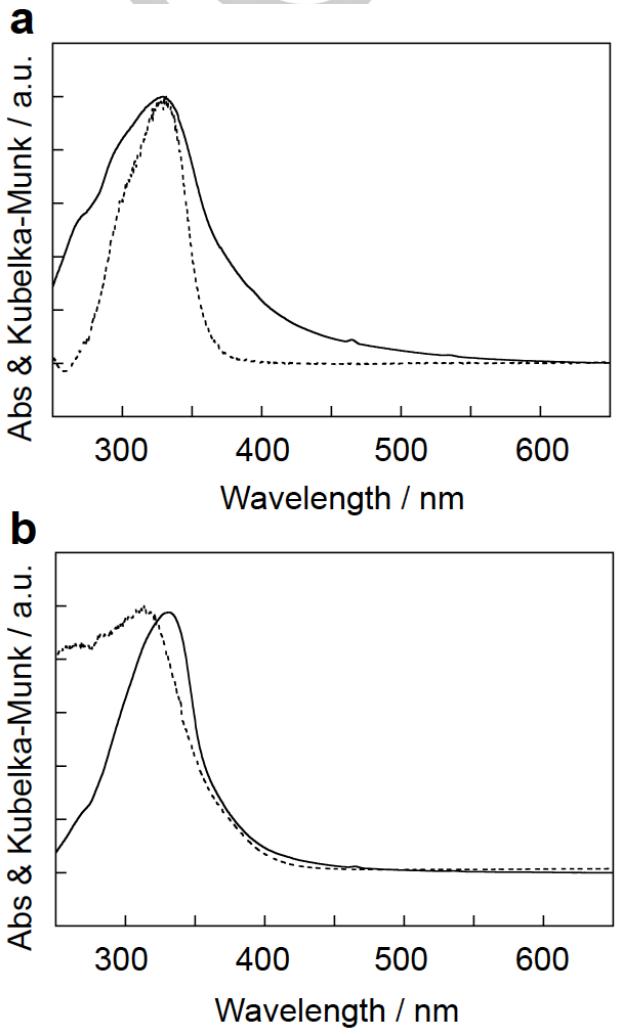

Figure 4. Diffuse reflectance spectra of $[Eu_3(hfa)_9(tppb)_2]_n$ (a: solid line), tppb (a: dashed line), $[Eu_3(hfa)_9(tpptz)_2]_n$ (b: solid line), and tpptz (b: dashed line) in solid state.

The steady-state emission spectra of $[Eu_3(hfa)_9(tppb)_2]_n$ and $[Eu_3(hfa)_9(tpptz)_2]_n$ in the solid state are shown in Figure 5a. The wavelength dependence of the detector response and the

beam intensity of the Xe light source for the each emission spectrum are calibrated using a standard light source. Emission bands for the Eu^{III} coordination polymers are observed at around 578, 592, 613, 650, and 698 nm, and are attributed to the 4*f*–4*f* transitions of $^5D_0$–^7F_J with J = 0, 1, 2, 3 and 4, respectively. The spectra are normalized with respect to the magnetic dipole transition intensities at 592 nm (Eu: $^5D_0$–$^7F_1$), which is known to be insensitive to the surrounding environment of the lanthanide ions.[26] The time-resolved emission profiles of $[Eu_3(hfa)_9(tppb)_2]_n$ and $[Eu_3(hfa)_9(tpptz)_2]_n$ revealed single-exponential decays with lifetimes in the millisecond time scale (Figure 5b). The emission lifetimes were determined from the slopes of logarithmic plots of the decay profiles. The observed emission lifetimes (τ_{obs}) of $[Eu_3(hfa)_9(tppb)_2]_n$ and $[Eu_3(hfa)_9(tpptz)_2]_n$ were found to be 0.87 and 0.78 ms, respectively.

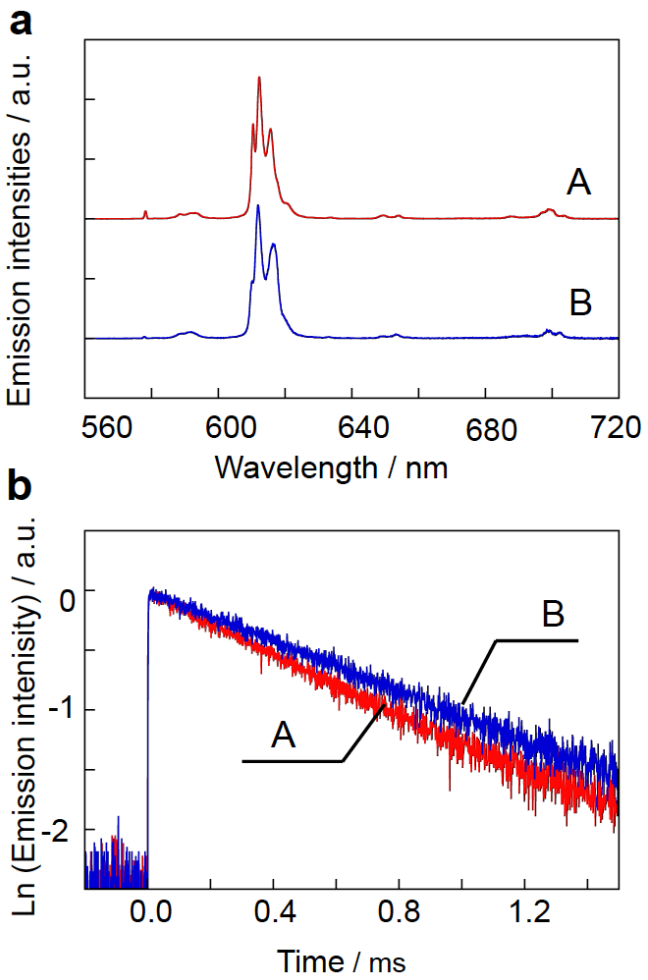

Figure 5. (a) Emission spectra of $[Eu_3(hfa)_9(tppb)_2]_n$ (A: red line) and $[Eu_3(hfa)_9(tpptz)_2]_n$ (B: blue line) in solid. Excited at 355 nm. (b) Emission decay profiles of $[Eu_3(hfa)_9(tppb)_2]_n$ (A: red line) and $[Eu_3(hfa)_9(tpptz)_2]_n$ (B: blue line).

The photosensitized emission efficiency ($\Phi_{\pi\text{-}\pi^*}$) of $[Eu_3(hfa)_9(tppb)_2]_n$ and $[Eu_3(hfa)_9(tpptz)_2]_n$ excited at 370 nm (π–π^* band of hfa ligand) using an integrating sphere (ϕ 100 mm) were estimated to be 64% and 38%, respectively, which are larger than that of the one-dimensional Eu^{III} coordination polymer $[Eu(hfa)_3(dpbp)]_n$ ($\Phi_{\pi\text{-}\pi^*}$ = 29%).

The emission quantum yields ($\Phi_{4f\text{-}4f}$), energy transfer efficiencies (η_{sens}), and radiative (k_r) and nonradiative (k_{nr}) rate constants for the Eu^{III} coordination polymers are shown in Table 1. The $\Phi_{4f\text{-}4f}$ of $[Eu_3(hfa)_9(tppb)_2]_n$ was estimated to be 82% in solid state, which is one of the best luminescence performances among Eu^{III} complexes and coordination polymers.[6] The $\Phi_{4f\text{-}4f}$ of $[Eu_3(hfa)_9(tpptz)_2]_n$ was found to be 78%. These high emission quantum yields are caused by small k_{nr} values of Eu^{III} coordination polymers with triangular spacers. The non-radiative rate constant k_{nr} is generally related to the thermal relaxation from the excited state, which is dependent on the vibrational structure of the luminescent materials. The remarkablely small k_{nr} constants of Eu^{III} coordination polymers with triangular spacers may be induced by the close stacking structure of the two-dimensional tppb and tpptz ligands in the crystals. The close packing structure of $[Eu_3(hfa)_9(tpptz)_2]_n$ might also produce an asymmetric coordination structure at around the Eu^{III} ions with molecular strain. In particular, the molecular strain in $[Eu_3(hfa)_9(tppb)_2]_n$ forms ILCT band and creates effective photosensitized energy efficiency ($[Eu_3(hfa)_9(tppb)_2]_n$: η_{sens} = 64%, $[Eu_3(hfa)_9(tpptz)_2]_n$: η_{sens} = 38%). The synergetic effect on the tight packing structure of Eu^{III} coordination polymers with rigid triangular spacers leads to an enhancement in structural stability, high emission quantum yield and effective energy transfer efficiency.

Triboluminescence properties

We observed TL of $[Eu_3(hfa)_9(tppb)_2]_n$ upon rubbing and crushing the crystals under an Ar atmosphere (Figure 6a). The TL spectrum of $[Eu_3(hfa)_9(tppb)_2]_n$ using a multi-channel high-speed spectro-analyzer (Hamamatsu Photonics PMA-11 multichannel analyzer) is shown in Figure 6a (the high-speed spectra are not calibrated using a standard light source). The high-speed detection system is different from the photomultiplier detection system with grating systems in Figure 5a. The spectral shape of the electric dipole transition band (613 nm: $^5D_0$–$^7F_2$ transition) of the TL spectrum (Figure 6a-A) was different from that of photoluminescence (Figure 6a-B, excited at 365 nm: UV-LED). We consider that the coordination symmetry of the luminescent Eu(III) center upon the breaking crystals by the rubbing process (TL) is different from that of photoluminescence of normal bulk crystals. In order to estimate the TL efficiency under an argon atmosphere, we introduced of shock wave irradiation using a nano-second laser pulse (Nd: YAG, λ = 1064 nm, fwhm = 5 nm, pulse energy = 0.1 mJ) for high-speed crushing of the crystals. The emission decay profile is shown in Figure 6b. We successfully observed the decay profile of TL of the Eu^{III} coordination polymer with triangular spacers, $[Eu_3(hfa)_9(tppb)_2]_n$. The decay profile revealed single-exponential decay with lifetime on the microsecond timescale. The TL lifetime is calculated to be 0.57 ms. The TL efficiency, k_r and k_{nr}, which are based on the TL spectrum and lifetime, are summarized in Table 1. The TL efficiency of $[Eu_3(hfa)_9(tppb)_2]_n$

was calculated to be 49%. The smaller k_r value for TL compared to photoluminescence indicates that the coordination symmetry of the triboluminescent Eu^{III} center is different from that of the photoluminescent Eu^{III} center. [28] The k_{nr} for triboluminescence is four times larger than that for photoluminescence in $[Eu_3(hfa)_9(tppb)_2]_n$ crystals, These results indicate that mechanical crushing of molecular crystals leads to enhancement of the non-radiative transition in the quantum process. We consider that the shock wave irradiation promotes effective mechanical crushing of organic crystals and the formation of the excited state of the ligands such as in the X-ray scintillation effect.[29]

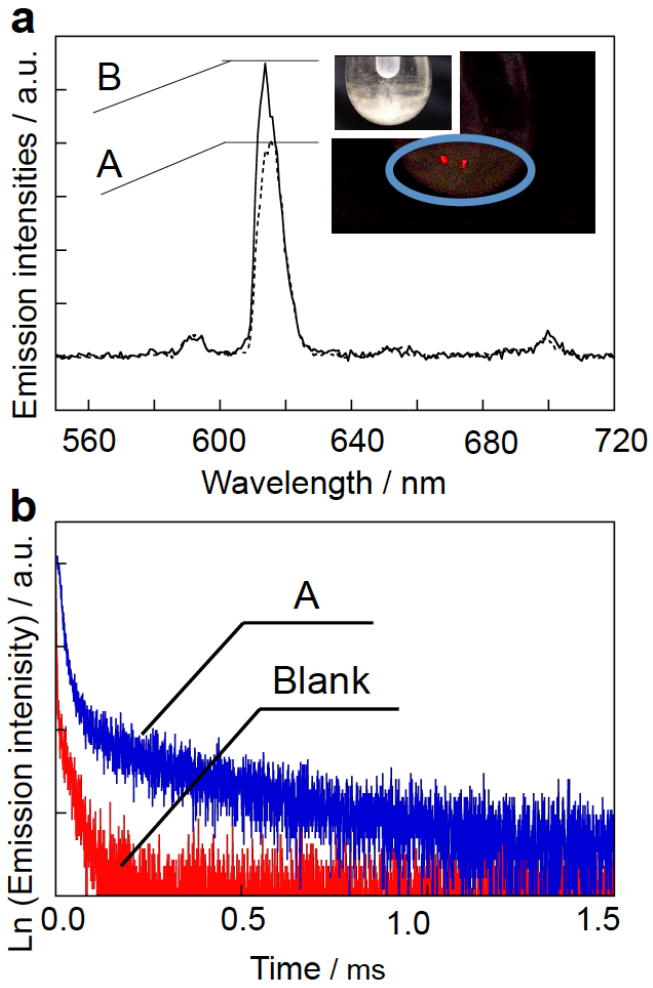

Figure 6. (a) Triboluminescence (A: dash line) and photoluminescence (B: bold line) spectra. Photoluminescence spectrum is observed by excitation at 355 nm. Inset: triboluminecence image of $[Eu_3(hfa)_9(tppb)_2]_n$. (b) emission decay profiles of triboluminescence of $[Eu_3(hfa)_9(tppb)_2]_n$ (A: blue line) and $BaSO_4$ powders (Blank: red line) under shock wave irradiation.

Conclusions

In this study, Eu^{III} coordination polymer $[Eu_3(hfa)_9(tppb)_2]_n$ with effective photo- and triboluminescence properties was performed for the first time. Successful observations were achieved using close packing structures of the Eu^{III} coordination polymer. The photosensitized luminescence efficiency $\Phi_{\pi\text{-}\pi^*}$ of $[Eu_3(hfa)_9(tppb)_2]_n$ excited at 355 nm was also found to be 64%, although we cannot observe TL from $[Eu_3(hfa)_9(tpptz)_2]_n$ ($\Phi_{\pi\text{-}\pi^*}$ = 38%) or $[Eu(hfa)_3(dpbp)]_n$ ($\Phi_{\pi\text{-}\pi^*}$ = 29%). Highly photosensitized luminescence efficiency for Eu^{III} coordination compound should be also key point for observation of triboluminescence. The effective molecular design and experimental analysis of two-dimensional luminescent lanthanide coordination polymers are expected to open-up a new frontier between coordination, material, and photophysical chemistry.

Table 1. Photophysical properties of Eu(III) coordination polymers in solid at room temperature

Coordination polymer	dp / °C	τ_{obs} /ms [a]	$\Phi_{\pi\text{-}\pi^*}$ / % [b]	$\Phi_{4f\text{-}4f}$ / % [c]	η_{sens} / % [c]	k_r / s^{-1}	k_{nr} / s^{-1}
$[Eu(hfa)_3(dpbp)]_n$ PL	308	0.85 ± 0.01	29	72	40	8.5×10^2	3.2×10^2
$[Eu_3(hfa)_9(tppb)_2]_n$ PL	354	0.87 ± 0.01	64	82	78	9.5×10^2	2.0×10^2
$[Eu_3(hfa)_9(tpptz)_2]_n$ PL	355	0.78 ± 0.01	38	78	48	1.1×10^3	2.7×10^2
$[Eu_3(hfa)_9(tppb)_2]_n$ TL[d]	354	0.57 ± 0.01[d]	-	49 [d]	-	8.7×10^2 [d]	8.9×10^2 [d]

PL: photoluminescence, TL: triboluminescence. [a] Emission lifetime (τ_{obs}) were measured by excitation at 355 nm (Nd: YAG, λ = 355 nm). [b] Emission quantum yields of photosentitized luminescence ($\Phi_{\pi\text{-}\pi^*}$□□ were determined by using integrating sphere. Excitation at 370 nm. [c] Emission quantum yields of 4*f*-4*f* transition of Eu(III) ions in Eu(III) coordination polymers were calculated (see results and discussion). [d] TL lifetime and spectrum were measured using near-infrared irradiation (Nd: YAG, λ = 1064 nm, pulse width = 5 nm, pulse energy = 0.1 mJ).

Experimental Section

Materials: Europium acetate monohydrate (99.9%) was purchased from Wako Pure Chemical Industries Ltd. 1,1,1,5,5,5-hexafluoro-2,4-pentanedione was obtained from Tokyo Kasei Organic Chemicals and Aldrich Chemical Company Inc. All other chemicals and solvents were reagent grade and were used without further purification.

Apparatus: Infrared spectra were recorded on a JASCO FT/IR–350 spectrometer. ^{1}H NMR (400 MHz) spectra were recorded on a JEOL ECS400. Chemical shifts are reported in □ ppm, referenced to an internal tetramethylsilane standard for ^{1}H NMR. IR spectra were measured using a JASCO FT/IR-350. Elemental analyses were performed using a Yanaco CNH corder MT-6. Mass spectrometry was performed with a JEOL JMS-T100LP. Thermogravimetric analysis (TGA) was performed on an SII EXSTAR-6000 analyzer.

Preparation of 4,4.-Bis(diphenylphosphoryl)biphenyl (dpbp): 4,4.-Bis-(diphenylphosphoryl)biphenyl was synthesized according to a published procedure[29]. A solution of *n*-BuLi (9.3 mL, 1.6M hexane, 15mmol) was added dropwise to a solution of 4,4.-dibromobiphenyl (1.9 g, 6.0mmol) in dry THF (30 mL) at –78°C. The addition was completed in

ca. 15 min during which time a yellow precipitate was formed. The mixture was stirred for 3 h, after which a PPh_2Cl (2.7 mL, 15mmol) was added dropwise at -78°C. The mixture was gradually brought to room temperature, and stirred for 14 h. The product was extracted with ethyl acetate, the extracts washed with brine three times and dried over anhydrous $MgSO_4$. The solvent was evaporated, and resulting residue was washed with acetone and ethanol several times. The obtained white solid and dichloromethane (ca. 40 mL) were placed in a flask. The solution was cooled to 0°C and then 30% H_2O_2 aqueous solution (5 mL) was added to it. The reaction mixture was stirred for 2 h. The product was extracted with dichloromethane, the extracts washed with brine three times and dried over anhydrous $MgSO_4$. The solvent was evaporated to afford a white powder. Recrystallization from dichloromethane gave white crystals of the titled compound (1.1 g, 33%). ^{1}H NMR (400 MHz, $CDCl_3$, 25°C): δ = 7.66-7.81 (m, 16H), 7.45-7.60 (m, 12H); IR(KBr): 1120 cm^{-1} (st, P=O); ESI-MS: *m/z* = 555.2 $[M+H]^+$; elemental analysis calcd (%) for $C_{36}H_{28}O_2P_2$: C 77.97, H 5.09; found: C 77.49, H 5.20.

Preparation of 1,3,5-tris(4-diphenylphosphorylphenyl) benzene (tppb): A solution of *n*-BuLi (7 mL, 1.6 M hexane, 11 mmol) was added dropwise to a solution of 1,3,5-tris(4-bromophenyl)benzene (2.0 g, 3.7 mmol) in dry THF (40 mL) at –78°C. The addition was completed in ca. 10 min during which time a white yellow precipitate was formed. The mixture was stirred for 2 h at –10°C, after which a PPh_2Cl (2 mL, 11 mmol) was added dropwise at –78°C. The mixture was gradually brought to room temperature, and stirred for 18 h. After the reaction, the product was extracted with dichloromethane (30 ml × 3), and then washed with brine for three times. The dichloromethane solution was dried using anhydrous $MgSO_4$ and concentrated to dryness. The obtained white powder and dichloromethane (ca. 30 mL) were placed in a flask. The solution was cooled to 0°C and then 30% H_2O_2 aqueous solution (8 mL) was added to it. The reaction mixture was stirred for 2 h. The product was extracted with dichloromethane, the extracts washed with brine for three times and dried over anhydrous $MgSO_4$. The solvent was evaporated to afford a white powder. The crude materials were separated using a silica-gel chromatography (methanol / ethyl acetate 1:5), and titled compound was recovered as a white solid (0.72 g, 28%). ^{1}H NMR (400 MHz, $CDCl_3$, 25°C): δ = 7.67-7.83 (m, 27H), 7.53-7.61 (m, 6H), 7.45-7.53 (m, 12H); IR (KBr): 1190 cm^{-1} (st, P=O); ESI–MS: *m/z* = 906.26 $[M]^+$; elemental analysis calcd (%) for $C_{60}H_{45}O_3P_3$: C 77.91, H 5.12; found: C 78.32, H 5.04.

Preparation of 2,4,6-tris(4-diphenylphosphorylphenyl-phenyl)-1,3,5-triazine (tpptz): The 2,4,6-tris(4-bromophenyl)-1,3,5-triazine (0.2, 0.37 mmol) and tetrakis(triphenylphosphine)palladium(0) (14 mg, 0.012 mmol) were added into a 5 ml of DMF under argon. Triethylamine (0.2 ml, 1.4 mmol) and diphenylphosphine (0.22 ml, 1.3 mmol) were added into the DMF solution. The reaction mixture was heated to 130˚C for 24 h. After the reaction, the product was extracted with dichloromethane (30 ml × 3), and then washed with brine for three times. The dichloromethane solution was dried using anhydrous $MgSO_4$ and concentrated to dryness. The obtained white powder and dichloromethane (ca. 30 mL) were placed in a flask. The solution was cooled to 0°C and then 30% H_2O_2 aqueous solution (8 mL) was added to it. The reaction mixture was stirred for 2 h. After the reaction, the product was extracted with dichloromethane (30 ml × 3), and then washed with brine for three times. The dichloromethane solution was dried using anhydrous $MgSO_4$ and concentrated to dryness. The crude materials were separated using a silica-gel chromatography (methanol / ethyl acetate 1:5), and titled compound was recovered as a white solid (0.14 g, 43%). ^{1}H NMR (400 MHz, $CDCl_3$, 25°C): δ = 8.79-8.84 (d, 6H), 7.85-7.94 (dd, 6H), 7.67–7.75 (m, 12H), 7.44–7.62 (m, 18H); IR (KBr): 1573-1369 cm^{-1} (st, C=N), 1180 cm^{-1} (st, P=O); ESI-MS: *m/z* = 910.25 $[M+H]^+$; elemental analysis calcd (%) for $C_{57}H_{42}N_3O_3P_3 + C_4H_8O_2$ (ethyl acetate): C 73.41, H 5.05, N 4.21; found: C 73.34, H 4.61, N 4.34.

Preparation of Tris(hexafluoroacetylacetonato)euro-pium Dihydrates $[Eu(hfa)_3(H_2O)_2]$: Europium acetate monohydrate (5.0 g, 13 mmol) was dissolved in distilled water (20 mL) in a 100 mL flask. A solution of 1,1,1,5,5,5-hexafluoro-2,4-pentanedione (7.0 g, 34 mmol) was added dropwise to the solution. The reaction mixture produced a precipitation of white yellow powder after stirring for 3 h at room temperature. The reaction mixture was filtered, and the resulting powder was recrystallized from methanol/water to afford colorless needle crystals of the titled compound (9.6 g, 95%). IR (KBr): 1650 cm^{-1} (st, C=O), 1145□1258 cm^{-1} (st, C–F); elemental analysis calcd (%) for $C_{15}H_7EuF_{18}O_8$ (809.91): C 22.27, H 0.87; found: C 22.12, H 1.01.

Preparations of $[Eu(hfa)_3(dpbp)]_n$ coordination polymer: The dpbp ligand (120 mg, 0.22 mmol) and $[Eu(hfa)_3(H_2O)_2]$ (178 mg, 0.22 mmol) were dissolved in methanol (20 mL). The solution was refluxed while stirring for 8 h, and the reaction mixture was concentrated to dryness. The resulting powder was washed with chloroform for several times. The powder was dried to afford a white powder. A single crystal suitable for X-ray structural determination of Eu^{III} coordination polymer was obtained by the diffusion method of methanol–chloroform solution at room temperature. $[Eu(hfa)_3(dpbp)]_n$ (196 mg, 67%; for monomer). IR (KBr): 1653 cm^{-1} (st, C=O), 1255-1145 cm^{-1} (st, C–F), 1127 cm^{-1} (st, P=O); ESI-MS: *m/z* = 1120.08 $[Eu(hfa)_2(dpbp)]^+$, 2447.15 $[Eu_2(hfa)_5(dpbp)_2]^+$; elemental analysis calcd (%) for $[C_{51}H_{31}EuF_{18}O_8P_2]_n$: C 46.14, H 2.35; found: C 45.59, H 2.49.

Preparations of $[Eu_3(hfa)_9(tppb)_2]_m$ coordination polymer: The tppb ligand (200 mg, 0.22 mmol) and $[Eu(hfa)_3(H_2O)_2]$ (534 mg, 0.66 mmol) were dissolved in methanol (20 mL). The solution was refluxed while stirring for 6 h, and the reaction mixture was concentrated to dryness. The resulting powder was washed with chloroform for several times. The powder was dried to afford a white powder (310 mg, 82%; for monomer). IR (KBr): 1650 cm^{-1} (st, C=O), 1625-1575 cm^{-1} (st, C-C), 1300-1230 cm^{-1} (st, C-F), 1150 cm^{-1} (st, P=O); ESI-MS: *m/z* = 1410.13 $[Eu(hfa)_2(tppb)]^+$, 2379.40 $[Eu(hfa)_2(tppb)_2]^+$, 3286.62 $[Eu(hfa)_2(tppb)_3]^+$, 4059.45 $[Eu_2(hfa)_5(tppb)_3]^+$, 4833.38 $[Eu_3(hfa)_8(tppb)_3]^+$; elemental analysis calcd (%) for $[C_{165}H_{99}Eu_3F_{54}O_{24}P_6]_n$: C 47.95, H 2.41; found: C 47.73, H 2.30.

Preparations of $[Eu_3(hfa)_9(tpptz)_2]_n$ coordination polymer: The tpptz ligand (200 mg, 0.22 mmol) and $[Eu(hfa)_3(H_2O)_2]$ (534 mg, 0.66 mmol) were dissolved in methanol (20 mL). The solution was refluxed while stirring for 6 h, and the reaction mixture was concentrated to dryness. The resulting powder was washed with chloroform for several times. The powder was dried to afford a white powder. (310 mg, 82%; for monomer). IR (KBr): 1655 cm^{-1} (st, C=O), 1595-1439 cm^{-1} (st, C-N), 1255 cm^{-1} (st, C-F), 1200 cm^{-1} (st, P=O); ESI-MS: *m/z* = 1476.12 $[Eu(hfa)_2(tpptz)]^+$, 2249.49 $[Eu_2(hfa)_5(tpptz)]^+$, 3024.91 $[Eu_3(hfa)_8(tpptz)_3]^+$, 3933.07 $[Eu_3(hfa)_8(tpptz)_2]^+$; elemental analysis calcd (%) for $[C_{159}H_{93}Eu_3F_{54}N_6O_{24}P_6]_n$: C 46.14, H 2.26, N 2.03; found: C 46.20, H 2.21, N 2.60. We consider that the elemental analysis is affected by small amount of terminal excess units tpptz on the crystal surface.

Optical Measurements: Absorption and emission spectra of the lanthanide complexes were measured with a JASCO V-670 spectrophotometor, JASCO F-6300-H spectrometer and Horiba Fluorolog spectrometers, which corrected for the response of the detector system. The emission quantum yields excited at 370 nm ($\Phi_{\pi\text{-}\pi^*}$) were estimated using a JASCO F-6300-H spectrometer attached with JASCO ILF-53 integrating sphere unit (φ = 100 nm). The wavelength dependence of the detector response and the beam intensity of the Xe light source for each spectrum were calibrated using a standard light source. The emission

spectra are normalized with respect to the magnetic dipole transition intensities at 592 nm (Eu: $^5D_0$–$^7F_1$), which are known to be insensitive to the surrounding environment of the lanthanide ions. Emission lifetimes of lanthanide coordination polymers were measured using the third harmonics (355 nm) of a Q-switched Nd: YAG laser (Spectra Physics, INDI-50, fwhm = 5 ns, λ = 1064 nm) and a photomultiplier (Hamamatsu Photonics, R5108, response time ≤ 1.1 ns). The Nd:YAG laser response was monitored with a digital oscilloscope (Sony Tektronix, TDS3052, 500 MHz) synchronized to the single-pulse excitation. Emission lifetimes were determined from the slope of logarithmic plots of the decay profiles. The TL spectrum of $[Eu_3(hfa)_9(tppb)_2]_n$ using multi-channel high-speed spectro-analyzer (HAMAMATSU photonics multichannel analyzer PMA-11). The decay profile of triboluminescence of $[Eu_3(hfa)_9(tppb)_2]_n$ were measured using nano-second laser pulse (Nd:YAG, λ = 1064 nm, fwhm = 5 nm, pulse energy = 0.1 mJ) for high-speed crushing of the crystals.

Calculation of the emission quantum yields: The 4*f*-4*f* emission quantum yields ($\Phi_{4f\text{-}4f}$), and the radiative (k_r) and nonradiative (k_{nr}) rate constants were estimated (Table 1) using following equations,

$$\tau_{rad} = \frac{1}{k_r} \quad (1)$$

$$\tau_{obs} = \frac{k_r}{k_r + k_{nr}} \quad (2)$$

$$\Phi_{4f-4f} = \frac{k_r}{k_r + k_{nr}} = \frac{\tau_{obs}}{\tau_{rad}} \quad (3)$$

$$k_r = A_{MD,0} n^3 \left(\frac{I_{tot}}{I_{MD}}\right) \quad (4)$$

$$k_{nr} = \frac{1}{\tau_{obs}} - \frac{1}{\tau_{rad}} \quad (5),$$

where $A_{MD,0}$ is the spontaneous emission probability for the $^5D_0$-$^7F_1$ transition in vacuo (14.65 s^{-1}), n is the refractive index of the medium (an average index of refraction equal to 1.5 was employed), and (I_{tot} / I_{MD}) is the ratio of the total area of the corrected Eu^{III} emission spectrum to the area of the $^5D_0$-$^7F_1$ band.

Acknowledgements

This work was partly supported by Grants-in-Aid for Scientific Research on Innovative Areas of “New Polymeric Materials Based on Element-Blocks (No. 2401)” (24102012) of the Ministry of Education, Culture, Sports, Science and Technology (MEXT) of Japan.

Keywords: europium • complex • luminescence • triboluminescence • coordination polymer

[1] H. Li, M. Eddaoudi, M. O'Keeffe, O. M. Yaghi, *Nature*, **1999**, *402*, 276-279.
[2] B. Moulton, M. J. Zaworotko, *Chem. Rev.*, **2001**, *101*, 1629-1658.
[3] S. L. James, *Chem. Soc. Rev.*, **2003**, *32*, 276-288.
[4] S. Kitagawa, R. Kitaura, S. Noro, *Angew. Chem. Int. Ed.*, **2004**, *43*, 2334-2375.
[5] I. G. Georgiev, L. R. MacGillivray, *Chem. Soc. Rev.*, **2007**, *36*, 1239-1248.
[6] Y. Hasegawa, T. Nakanishi, *RSC Adv.*, **2015**, *5*, 338-353.
[7] V. Haquin, M. Etienne, C. Daiguebonne, S. Freslon, G. Calvez, K. Bernot, L. Le Poll`es, S. E. Ashbrook, M. R. Mitchell, J.-C. Bünzli, S. V. Eliseeva, O. Guillou, *Eur. J. Inorg. Chem.*, **2013**, *2013*, 3464-3476.
[8] K. Miyata, Y. Konno, T. Nakanishi, A. Kobayashi, M. Kato, K. Fushimi, Y. Hasegawa, *Angew. Chem. Int. Ed.*, **2013**, *52*, 6413-6416.
[9] C. Daiguebonne, N. Kerbellec, O. Guillou, J.-C. Bünzli,F. Gumy, L. Catala, T. Mallah, N. Audebrand, Y. G´erault, K. Bernot, G. Calvez, *Inorg. Chem*., **2008**, *47*, 3700-3708.
[10] A. de Bettencourt-Dias, *Inorg. Chem*., **2005**, *44*, 2734-2741.
[11] H.-S. Wang, B. Zhao, B. Zhai, W. Shi, P. Cheng, D.-Z. Liao, S.-P. Yan, *Cryst. Growth Des.*, **2007**, *7*, 1851-1857.
[12] K. Miyata, T. Ohba, A. Kobayashi, M. Kato, T. Nakanishi, K. Fushimi, Y. Hasegawa, *ChemPlusChem*, **2012**, *77*, 277-280.
[13] Y. Hasegawa, Y. Kimura, K. Murakoshi, Y. Wada, J.-H. Kim, N. Nakashima, T. Yamanaka, S. Yanagida, *J. Phys. Chem*., **1996**, *100*, 10201-10205.
[14] J. I. Zink, *Accounts Chem. Res.*, **1978**, *11*, 289-295.
[15] A. J. Walton, *Adv. Phys.*, **1977**, *26*, 887-948.
[16] Y. C. Miranda, L. L. A. L. Pereira, J. H. P. Barbosa, H. F. Brito, M. C. F. C. Felinto, O. L. Malta, W. M. Faustino, E. E. S. Teotonio, *Eur. J. Inorg. Chem*., **2015**, *2015*, 3019-3027.
[17] S. Biju, Gopakumar, J.-C. G. Bünzli, R. Scopelliti, H. K. Kim, M. L. P. Reddy, *Inorg. Chem*., **2013**, *52*, 8750-8758.
[18] E. A. Mikhalyova, A. V. Yakovenko, M. Zeller, M. A. Kiskin, Y. V. Kolomzarov, I. L. Eremenko, A. W. Addison, V. V. Pavlishchuk, *Inorg. Chem.*, **2015**, *54*, 3125-3133.
[19] Y. Hasegawa, R. Hieda, K. Miyata, T. Nakagawa, T. Kawai, *Eur. J. Inorg. Chem.*, **2011**, *2011*, 4978-4984.
[20] S. V. Eliseeva, D. N. Pleshkov, K. A. Lyssenko, L. S. Lepnev, J.-C. G. Bünzli, N. P. Kuzmina, *Inorg. Chem.*, **2010**, *49*, 9300-9311.
[21] X.-F. Chen, X.-H. Zhu, Y.-H. Xu, S. S. S. Raj, S. Öztürk, H.-K. Fun, J. Ma, X.-Z. You, *J. Mater. Chem.*, **1999**, *9*, 2919-2922.
[22] M. H. V. Werts, R. T. F. Jukes, J. W. Verhoeven, *Phys. Chem. Chem. Phys.*, **2002**, *4*, 1542-1548.
[23] A. Aebischer, F. Gumy, J.-C. G. Bunzli, *Phys. Chem. Chem. Phys.*, **2009**, *11*, 1346-1353.
[24] Y. Tsuboi, T. Seto, N. Kitamura, *J. Phys. Chem. A*, **2008**, *112*, 6517-6521.
[25] S. Naik, M. Kumaravel, J. T. Mague, M. S. Balakrishna, *Inorg. Chem.*, **2014**, *53*, 1370-1381.
[26] Y. Hasegawa, M. Yamamuro, Y. Wada, N. Kanehisa, M. Kai S. Yanagida, *J. Phys. Chem. A*, **2003**, *107*, 1697-1702.
[27] S. V. Eliseeva, O. V. Kotova, F. Gumy, S. N. Semenov, V. G. Kesler, L. S. Lepnev, J.-C. G. Bünzli, N. P. Kuzmina, *J. Phys. Chem. A*, **2008**, *112*, 3614-3626.
[28] K. Miyata, T. Nakagawa, R. Kawakami, K. Kita, K. Sugimoto, T. Nakashima, T. Harada, T. Kawai, Y. Hasegawa, *Chem. Eur. J.*, **2011**, *17*, 521-528.
[29] P. N. Zhmurin, V. N. Lebedev, A. F. Adadurov, V. N. Pereymak, Y. A. Gurkalenko, *Radiat. Meas.*, **2014**, *62*, 1-5.

Entry for the Table of Contents

Layout 1:

FULL PAPER

Luminescent Eu^{III} coordination polymers with trianglar spacer ligands are reported. Characteristic thermo-stable sheet-stacked structure, high emission quantum yield ($\Phi_{4f\text{-}4f}$ = 82%), effective photosensitized energy transfer (η_{sens} = 78%) and remarkable triboluminescence properties of Eu(III) coordination polymers with trianglar spacers are demonstrated.

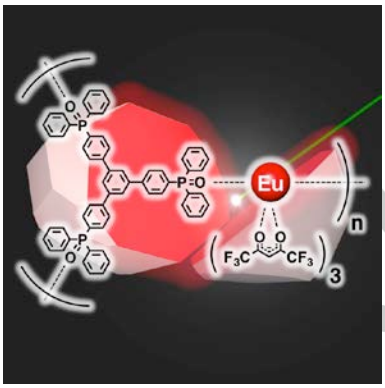

Lanthanide, luminescence*

Yasuchika Hasegawa, Shiori Tateno, Masanori Yamamoto, Takayuki Nakanishi, Yuich Kitagawa, Tomohiro Seki, Hajime Ito, Koji Fushimi*

Page No. – Page No.

Effective Photo- and Triboluminescent Eu^{III} Coordination Polymers with rigid triangular spacer ligands

*one or two words that highlight the emphasis of the paper or the field of the study